

## Supporting information

### **Narcissistic Self-Sorting in Zn(II) Porphyrin Derived Semiconducting Nanostructures**

Yelukula Ramakrishna,<sup>a,b</sup> Madarapu Naresh,<sup>a,b</sup> Madoori Mrinalini,<sup>\*a,b,c</sup> Nagadatta Pravallika,<sup>a</sup> Priti Kumari,<sup>a</sup> Botta Bhavani,<sup>a,b</sup> Lingamallu Giribabu,<sup>a,b</sup> Seelam Prasanthkumar<sup>\*a,b</sup>

*<sup>a</sup>Department of Polymer & Functional Materials, CSIR-Indian Institute of Chemical Technology (IICT), Tarnaka, Hyderabad-500007, Telangana, India*

*<sup>b</sup>Academy of Scientific and Innovation Research (AcSIR), Ghaziabad-201 002, India.*

*<sup>c</sup>Materials Chemistry Department, CSIR- Institute of Minerals and Materials Technology (IMMT), Bhubaneswar - 751 013, Odisha, INDIA*

Corresponding Author E-mail: [mabani1n@gmail.com](mailto:mabani1n@gmail.com), [prasanth@iict.res.in](mailto:prasanth@iict.res.in)

## Table of contents

1. Experimental details.....	S3-S5
2. Synthesis of <b>PA</b> and <b>PB</b> .....	S6-S8
3. <sup>1</sup> H NMR spectra of <b>PA</b> and <b>PB</b> .....	S8-S9
4. <sup>13</sup> C NMR spectra of <b>PA</b> and <b>PB</b> .....	S9-S10
5. MALDI-TOF-MS Spectra.....	S10-S11
6. Photophysical data of <b>PA</b> , <b>PB</b> and <b>PA+PB</b> in solution state.....	S11
7. <sup>1</sup> H NMR spectral studies of <b>PA</b> , <b>PB</b> and <b>PA+PB</b> .....	S12
8. NOESY Spectra of <b>PA</b> , <b>PB</b> and <b>PA+PB</b> .....	S12-S13
9. FT-IR studies of <b>PA</b> , <b>PB</b> and <b>PA+PB</b> in chloroform.....	S14
10. Electrochemistry studies of <b>PA</b> , <b>PB</b> and <b>PA+PB</b> .....	S14-S15
11. Emission studies of <b>PA</b> , <b>PB</b> , and <b>PA+PB</b> .....	S16-S17
12. Microscopic analysis of <b>PA+PB</b> .....	S17
12. Powder x-ray diffraction analyses of <b>PA</b> , <b>PB</b> and <b>PA+PB</b> derivatives.....	S18
13. Electrochemical impedance analysis of <b>PA</b> , <b>PB</b> and <b>PA+PB</b> derivatives.....	S19-S20
14. References.....	S21

## 1. Experimental details

**Materials:** Chemicals and reagents that were readily available for purchase were obtained from Merck or Sigma-Aldrich. Laboratory reagent (LR) grade solvents were used for column chromatography and sample purification, while analytical reagent (AR) grade solvents were utilized for the reactions. Column chromatography was performed using ACME silica gel (100–200 mesh). Merck based Silica gel 60-F254 plates that had been precoated were used for thin layer chromatography. To purify every compound, either flash chromatography or gravity chromatography was used. All of the reactions used dry, degassed solvents and were conducted in either an argon or nitrogen atmosphere.

**Characterization Techniques:** Matrix-assisted laser desorption ionization time-of-flight (MALDI–TOF) mass spectrometry of **PA** and **PB** was performed on Shimadzu Biotech Axima Performance 2.9.3.20110624: Mode Reflectron-HiRes, Power: 85. <sup>1</sup>H Nuclear magnetic resonance (NMR) and <sup>13</sup>C spectra of samples were recorded on a 500 MHz INOVA spectrometer using CDCl<sub>3</sub> as an internal reference.

**UV-visible and Fluorescence Measurements:** UV-vis absorption spectra of **PA**, **PB** and **PA+PB** were recorded in chloroform and cyclohexane solvents on Shimadzu (Model UV-3600) spectrophotometer. All the analyses were performed in CHCl<sub>3</sub> and cyclohexane in a 1 cm cuvette at a concentration of 1 × 10<sup>-5</sup> M. Three samples exhibit monomeric species in chloroform and aggregates in cyclohexane under the heating-cooling procedure. Subsequently, temperature dependent UV-visible absorption spectroscopic analyses were performed for three samples (**PA**, **PB** and **PA+PB**) in cyclohexane with increasing the temperature from 20 °C to 70 °C with the time intervals of 10 °C. Furthermore, the fractions of aggregated species ( $\alpha$ ) were calculated from the temperature dependent UV-visible absorption spectroscopic analyses of three samples by following the below equation at the absorption maxima of 420 nm (soret band region).<sup>1</sup>

$$\alpha = (\epsilon_{\text{monomer}} - \epsilon) / (\epsilon_{\text{monomer}} - \epsilon_{\text{aggregates}}),$$

where  $\epsilon_{\text{aggregates}}$  and  $\epsilon_{\text{monomer}}$  were taken from fully aggregated spectra in cyclohexane and completely monomeric spectra in chloroform, respectively.

Steady-state fluorescence spectra of solutions were recorded on a Fluorolog-3 spectrofluorometer (Spex model, Jobin Yvon) at the wavelength of excitation ( $\lambda_{\text{exc}}$ ) = 420 and 470 nm. Photoluminescence decay profiles measured on a picoseconds time-

correlated single photon (TCSPC) setup (Fluorolog-3-Triple Illuminator, IBH Horiba Jobin Yvon) employing a picoseconds light emitting diode laser (Nano LED,  $\lambda_{\text{exc}} = 440$  nm).

**Fourier Transform Infrared Spectroscopy (FT-IR) Measurements:** FT-IR of **PA**, **PB** and **PA+PB** were recorded on a Thermo Nicolet Nexus 670 spectrometer with a resolution of  $4 \text{ cm}^{-1}$  and KBr as a beam splitter. For liquid samples, solution of three derivatives were prepared from chloroform and drop-casted between two disks of KBr and then placed into a pellet holder. Whereas, aggregates of **PA**, **PB** and **PA+PB** were prepared by heating the samples until dissolve in cyclohexane and subsequent cooling method. The obtained aggregates were dropped onto the KBr disc and recorded the spectra at  $25 \text{ }^\circ\text{C}$ .

**Electrochemical Studies:** Cyclic voltammetry experiments of **PA**, **PB** and **PA+PB** were performed on a PC-controlled CH instruments model CHI 620C electrochemical analyzer in  $\text{CHCl}_3$  at a scan rate of  $200 \text{ mV/s}$  using  $0.1 \text{ M}$  tetrabutylammonium hexafluorophosphate ( $\text{NBu}_4\text{PF}_6$ ) before and after exposure to UV light. The working electrode is glassy carbon, the saturated calomel electrode (SCE) is the reference electrode and the platinum wire is an auxiliary electrode. Subsequently, Spectro electrochemistry of both derivatives was measured using maximum oxidation and reduction potentials and recorded absorption spectral variation under different redox potentials.

**Powder X-ray Diffraction (PXRD) Analysis:** PXRD studies were accomplished by transferring the aggregates of **PA**, **PB** and **PA+PB** onto a glass slide and drying slowly. The excess solvent was removed by vacuum. X-ray diffractograms of the dried films were recorded on a Simens D5000 X-ray diffractometer using  $\text{Cu K}\alpha$  radiation.

**Microscopic Analysis:** Scanning electron microscopy (SEM) measurements of **PA**, **PB** and **PA+PB** were executed using FESEM (JEOL 7610F FESEM equipped with an OXFORD EDAX detector). Transmission electron microscopy (TEM) measurements were also measured using FEI Talos 120 KV. For measurements, samples were prepared from the cyclohexane using the heating–cooling technique and drop-casted aggregates on copper substrate and carbon-coated copper grids (200 mesh size) directly at  $25 \text{ }^\circ\text{C}$ . High-angle annular dark-field scanning transmission electron microscopy (HAADF-STEM) was performed using an electron beam with a relatively low accelerating voltage of  $120 \text{ kV}$ .

**Theoretical calculations:** Density functional theory (Gaussian 09 program package) with B3LYP 6-31g (d,p) level adopted for measuring the optimized structure and frontier molecular orbitals (FMOs) of **PA** and **PB**. Herein, all DFT calculations are run on zinc metal-based porphyrin-anthracene and porphyrin-benzothiadiazole molecular systems respectively. HOMO/LUMO energy levels, frontier molecular orbitals, and electrostatic potential (ESP) maps of the optimized structure were then generated using GaussView 5.0 and the formatted check files from the Gaussian 09 computation.

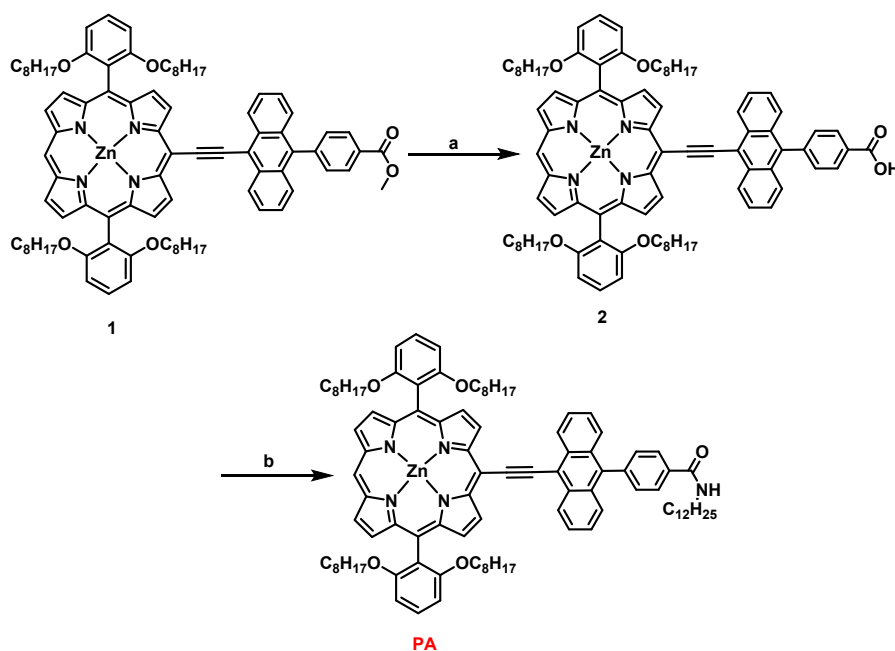
**Electrochemical Impedance Spectroscopy (EIS):** Sample preparation for the experiments was achieved by conducting indium tin oxide (ITO) substrates that provide inert electrical contacts. Selective etching of indium tin oxide (ITO) glass slides (1 cm × 1 cm) was performed using 1 M HCl/Zn dust on a masked pattern to prefabricate two parallel electrodes set at a distance of ~1.5 mm apart. The samples were then deposited as thin films of the **PA**, **PB** and **PA+PB** derivatives, and their corresponding aggregates were prepared at a concentration of  $1 \times 10^{-5}$  M in CHCl<sub>3</sub>/MeOH on pre-masked substrate with the dimensions of length-0.15 cm, width-0.20 cm and a thickness of 80 nm surface to achieve comparable and quantifiable cell geometry. Electrochemical impedance spectroscopy was performed on the deposited thin films employing a Zahner Zennium Electrochemical Workstation equipped with Thales operational software and coupled with a controlled heating chamber to carry out variable temperature measurements during heating. The measurements were carried out at different temperature settings from 20 °C - 80 °C with a stepwise increase in temperature of 10 °C. The temperature was measured with an accuracy higher than ±0.1 °C using a K-type thermocouple placed close to the sample. The samples were equilibrated at each temperature for 1 h before acquiring the frequency sweep impedance data. The data were collected following a frequency sweep through 100–500 Hz at an alternating potential with root-mean-square amplitude of ±10 mV across the open-circuit voltage (OCV) of the assembled cells.

**Preparation of aggregates by heating-cooling method:** PA + PB solution was prepared by a 1:1 molar ratio of PA and PB dissolved in chloroform and cyclohexane (heating method) which is in a monomeric state initially and then applied the heating-cooling method in cyclohexane to check the aggregation phenomenon. Since PA and PB are partially soluble in cyclohexane, we have done the heating of all samples until they are completely soluble and followed by cooling the solution. For the experiments, we have used a concentration of 10 μM for PA, PB and PA+PB (1:1 M) in chloroform and

cyclohexane. As a result, aggregates were formed and studied systematically using UV-visible absorption and emission spectroscopy, microscopic images, PXRD and electrochemical impedance analyses.

## 2. Synthesis of PA and PB:

### 2.1. Synthesis of PA:



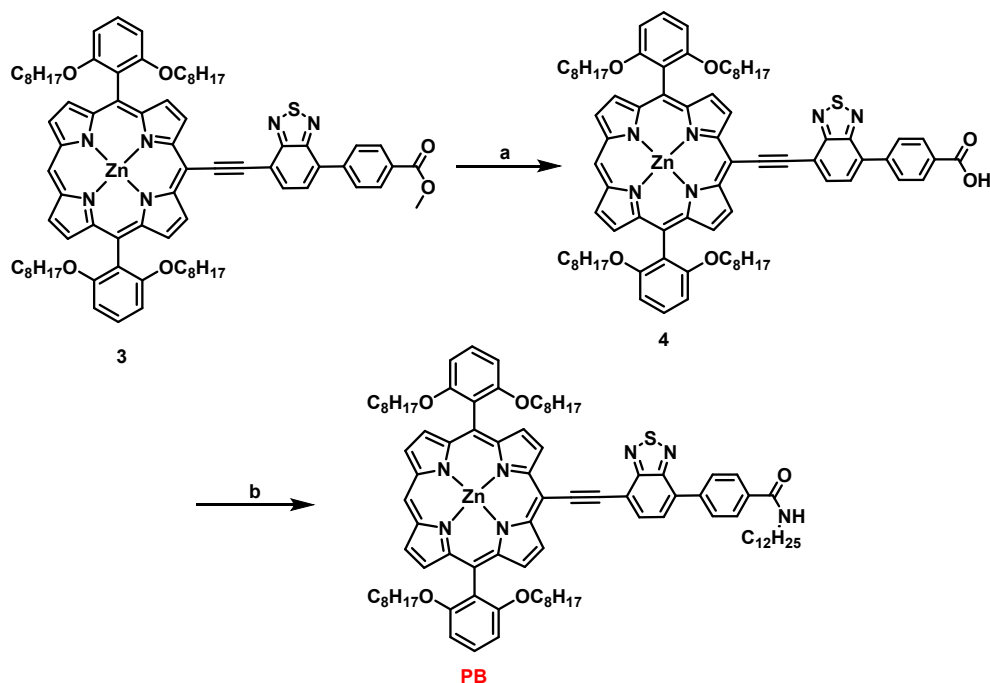
**Scheme S1.** Synthesis of PA. *Reagent and Conditions:* (a) LiOH, THF, 80 °C, 6 h,  $\text{N}_2$  atmosphere, yield: 60%. (c) HATU, DIPEA, THF: DCM (1:1 v/v), 12 h, 0 °C,  $\text{N}_2$  atmosphere, yield: 50%.

**Synthetic procedure for PA:** Compound **1** was synthesized using a known synthetic process.<sup>2-5</sup> LiOH (10.442 mg, 0.436 mmol),  $\text{H}_2\text{O}$  (10 mL), and 20 mL THF were added to compound **1** (150 mg, 0.109 mmol). The final reaction mixture was refluxed for six hours at 80 °C in a  $\text{N}_2$  atmosphere. The excess solvent was then removed under reduced pressure, and the mixture was then washed with a dichloromethane/water solution. In order to obtain compound **2**, the resulting organic layer was dried over  $\text{Na}_2\text{SO}_4$  and purified using column chromatography (silica gel: 100–200 mesh, DCM/Methanol). Then, compound **2** (100 mg, 0.073 mmol) was added to 30 mL of THF, 3 mL of dodecyl amine (0.182 mmol), and 5.55 mg (0.0140 mmol) of HATU was added while the reaction mixture was maintained at 0 °C in a  $\text{N}_2$  atmosphere.<sup>6</sup> Following a 10-minute duration, 1 mL of DIPEA (0.0140 mmol) was added, and TLC was used to track the reaction's advancement. Afterwards, the solvent was extracted

using low pressure, column chromatography (silica gel: 100 – 200 mesh, DCM/Methanol). Yield: 50 %.

**<sup>1</sup>H NMR** (400 MHz, CDCl<sub>3</sub>) δ: 10.39 – 9.94 (m, 1H), 9.43 (d, *J* = 8.6 Hz, 1H), 9.26 (d, *J* = 4.4 Hz, 1H), 9.08 (d, *J* = 4.6 Hz, 1H), 8.98 (d, *J* = 4.4 Hz, 1H), 8.01 (d, *J* = 7.8 Hz, 1H), 7.74 (dd, *J* = 15.7, 8.5 Hz, 2H), 7.63 (d, *J* = 7.9 Hz, 1H), 7.56 – 7.44 (m, 1H), 7.44 – 7.30 (m, 1H), 7.03 (d, *J* = 8.5 Hz, 2H), 6.27 (t, *J* = 5.3 Hz, 1H), 3.86 (t, *J* = 6.4 Hz, 3H), 3.53 (t, 1H), 1.27 (d, *J* = 12.6 Hz, 14H), 1.08 – 0.85 (m, 6H), 0.74 (dd, *J* = 14.6, 7.3 Hz, 4H), 0.47 (ddd, *J* = 20.6, 13.0, 6.5 Hz, 19H). **<sup>13</sup>C NMR** (151 MHz, CDCl<sub>3</sub>) δ: 176.15 (d, *J* = 95.2 Hz), 172.17 (s), 167.02 – 166.11 (m), 158.91 (d, *J* = 25.1 Hz), 151.28 (s), 145.68 (t, *J* = 175.2 Hz), 142.29 (s), 139.92 – 137.01 (m), 135.71 – 132.80 (m), 130.91 – 130.20 (m), 130.05 – 128.52 (m), 128.52 – 126.54 (m), 131.73 – 111.91 (m), 125.26 (ddd, *J* = 126.0, 57.3, 37.0 Hz), 123.65 – 122.03 (m), 118.07 (s), 114.88 (s), 113.06 (s), 104.38 (s), 68.28 – 65.95 (m), 62.03 (s), 38.52 (s), 35.95 (s), 30.94 (s), 28.65 (d, *J* = 4.1 Hz), 25.94 (s), 24.86 (s), 21.70 (s), 13.12 (s). **MALDI-TOF-MS** (m/z): 1526.95 (Calculated mass = 1526.47).

## 2.2 Synthesis of P-BDT(PB):



**Scheme S2. Synthesis of PB:** Reagent and Conditions: (a) LiOH, THF, 80 °C, 6 h, N<sub>2</sub> atmosphere, yield: 60%. (b) HATU, DIPEA, THF: DCM (1:1 v/v), 12 h, 0 °C, N<sub>2</sub> atmosphere, yield: 50%.

**Synthetic procedure:** Compound **PB** prepared from the similar synthetic procedure of **PA** using the reactant of dibromo-benzothiadiazole ester (yield: 50 %)

**<sup>1</sup>H NMR** (400 MHz, CDCl<sub>3</sub>) δ: 9.96 (d, *J* = 4.5 Hz, 2H), 9.87 (s, 1H), 9.07 (d, *J* = 4.4 Hz, 2H), 8.91 (d, *J* = 4.5 Hz, 2H), 8.79 (d, *J* = 4.4 Hz, 2H), 8.20 (t, *J* = 6.3 Hz, 1H), 8.06 (d, *J* = 8.3 Hz, 2H), 7.85 (dd, *J* = 16.4, 7.8 Hz, 3H), 7.63 (dd, *J* = 10.9, 6.0 Hz, 2H), 6.94 (d, *J* = 8.5 Hz, 4H), 6.10 (t, *J* = 5.6 Hz, 1H), 3.77 (t, *J* = 6.5 Hz, 8H), 3.44 (dd, *J* = 13.2, 6.9 Hz, 2H), 1.18 (s, 22H), 0.83 (dd, *J* = 6.3, 3.6 Hz, 13H), 0.75 (t, *J* = 7.1 Hz, 7H), 0.68 – 0.47 (m, 40H).

**<sup>13</sup>C NMR** (151 MHz, CDCl<sub>3</sub>) δ: 172.10 (s), 165.55 (d, *J* = 1979.5 Hz), 158.99 (s), 150.55 (d, *J* = 113.3 Hz), 154.37 – 145.01 (m), 148.14 – 145.62 (m), 141.76 (s), 138.75 (dd, *J* = 384.4, 267.4 Hz), 139.37 – 136.42 (m), 134.14 (s), 130.57 (s), 129.08 – 126.82 (m), 136.10 – 119.83 (m), 132.59 – 121.14 (m), 126.79 – 124.48 (m), 122.98 (dd, *J* = 77.7, 70.0 Hz), 118.08 (s), 113.97 (d, *J* = 275.4 Hz), 104.31 (s), 68.73 – 66.13 (m), 30.62 (s), 29.19 (s), 28.69 – 28.61 (m), 25.83 (d, *J* = 27.4 Hz), 24.19 (s), 21.70 (s), 13.13 (s). **MALDI-TOF-MS** (*m/z*) = 1483.89 (calculated mass = 1482.80).

### 3. <sup>1</sup>H NMR spectra of PA and PB derivatives:

#### 3.1. <sup>1</sup>H NMR spectra of PA:

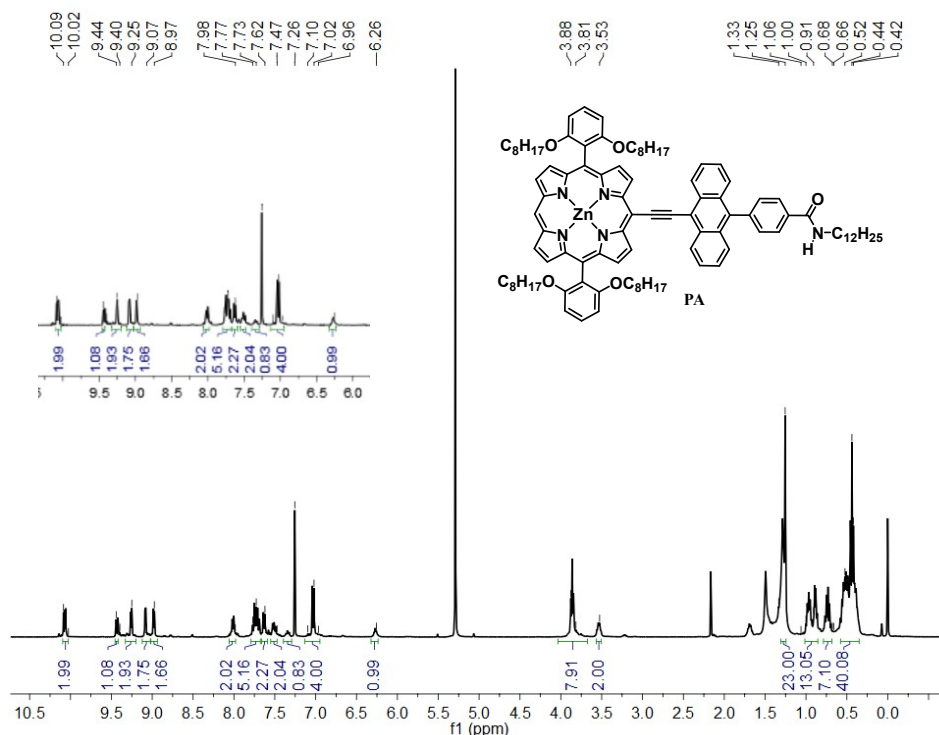


**Fig. S1** <sup>1</sup>H NMR Spectrum of **PA**.

### 3.2. <sup>1</sup>H NMR spectra of PB:

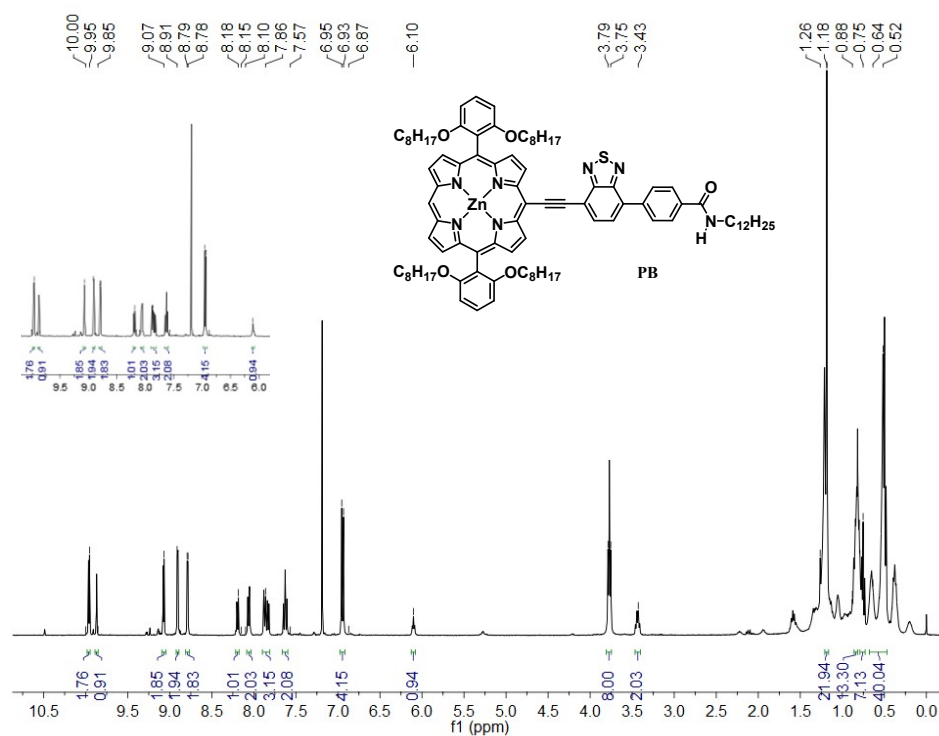


Fig. S2 <sup>1</sup>H NMR Spectrum of PA.

### 4. <sup>13</sup>C NMR spectra of PA and PB derivatives:

#### 4.1 <sup>13</sup>C NMR spectra of PA:

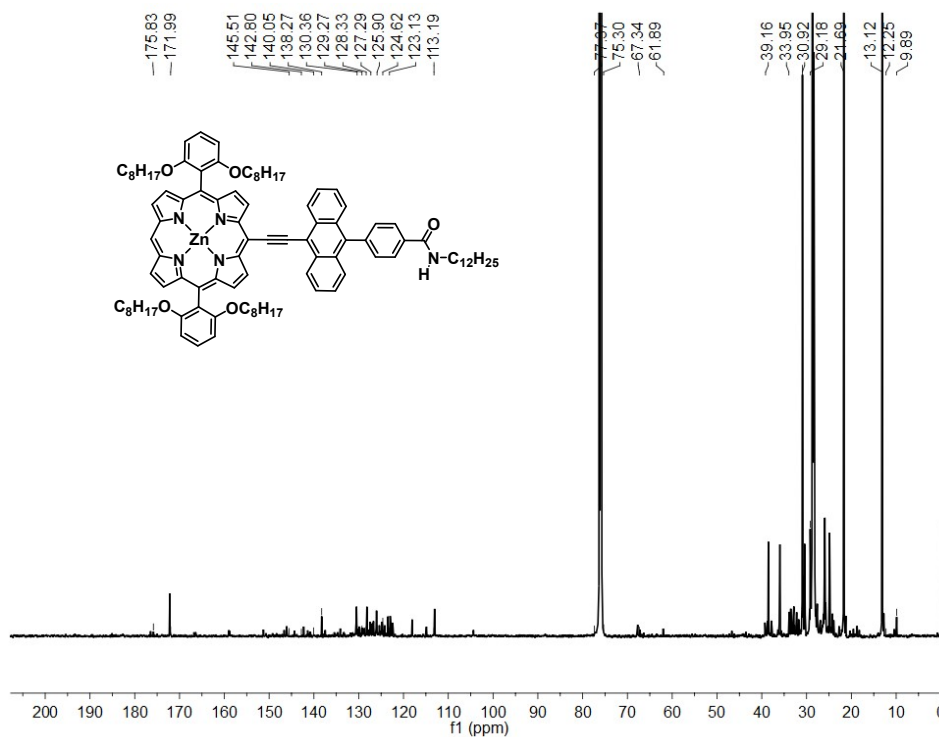


Fig. S3 <sup>13</sup>C NMR Spectrum of PA.

## 4.2 $^{13}\text{C}$ NMR spectra of P-BDT:

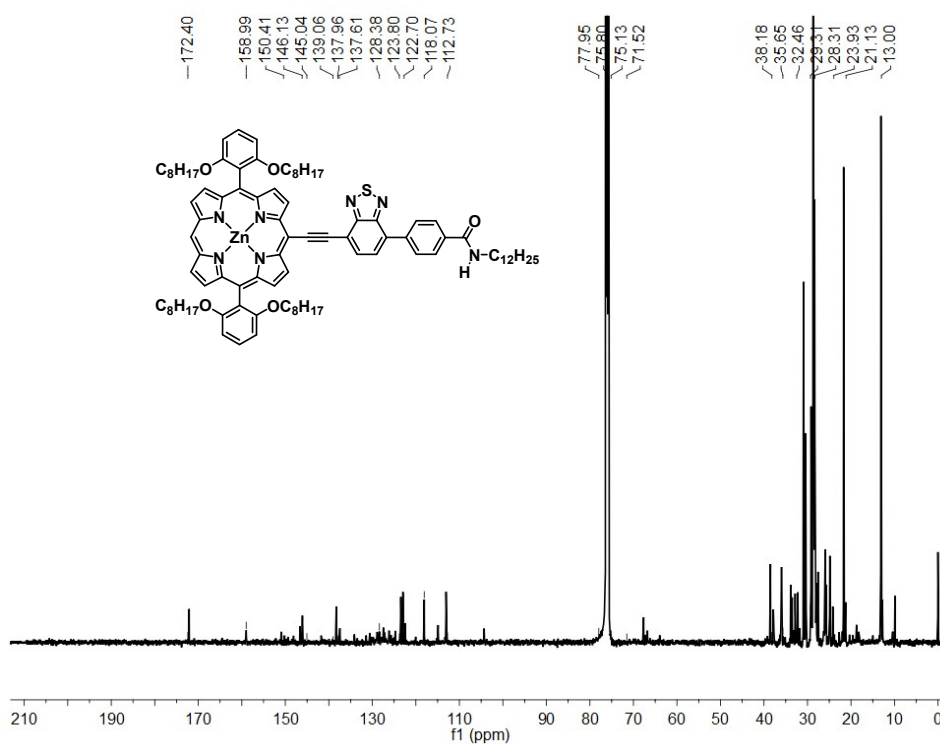


Fig. S4  $^{13}\text{C}$  NMR Spectrum of PB.

## 5. MALDI- TOF- MS spectra:

### 5.1 MALDI- TOF -MS spectra of PA:

MALDI-TOF-MS ( $m/z$ ) = 1526.95 (calculated mass = 1526.47).

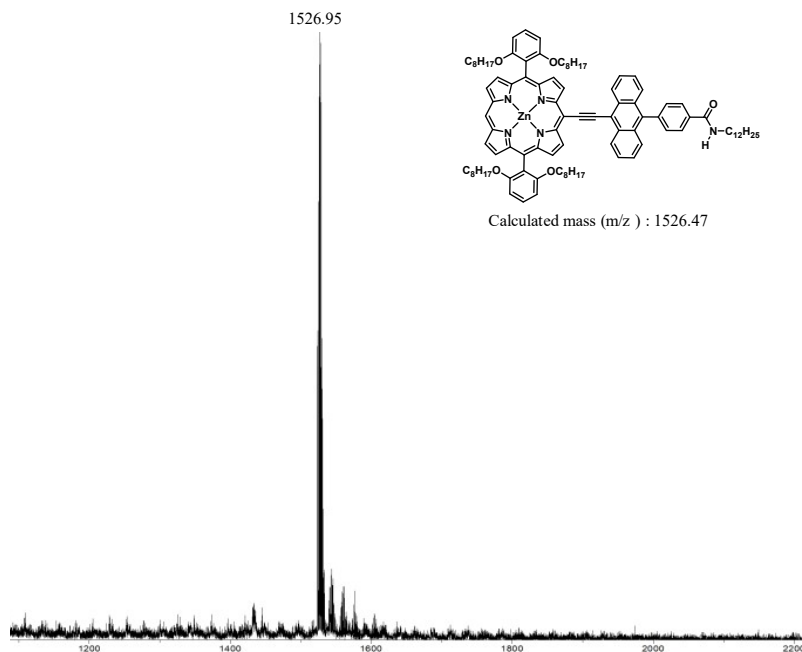
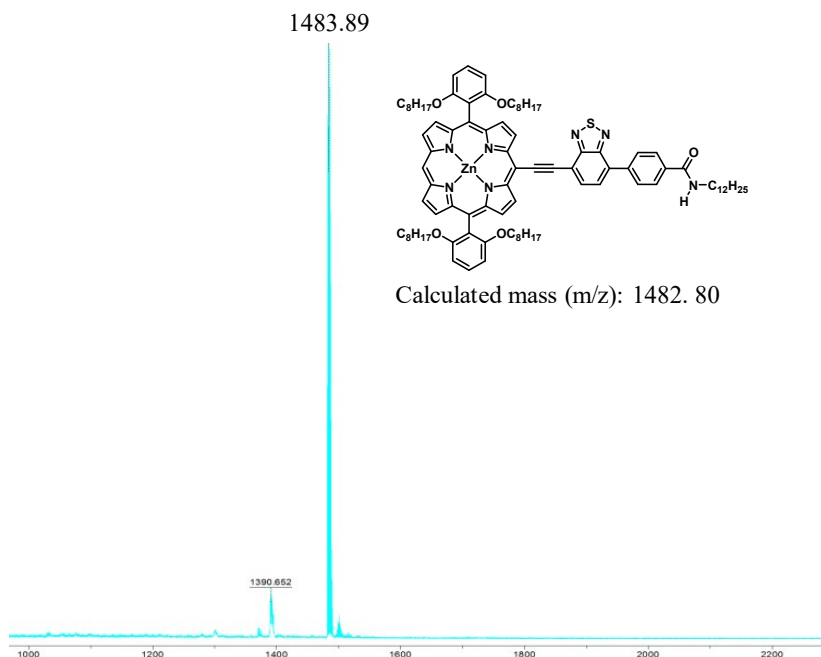


Fig. S5 MALDI-TOF-MS Spectrum of PA

## 5.2 MALDI- TOF -MS Spectra of PB:

MALDI-TOF-MS ( $m/z$ ) = 1483.89 (calculated mass = 1482.80).



**Fig. S6** MALDI-TOF MS Spectrum of PB.

## 6. Photophysical data of PA, PB and PA+PB in solution state:

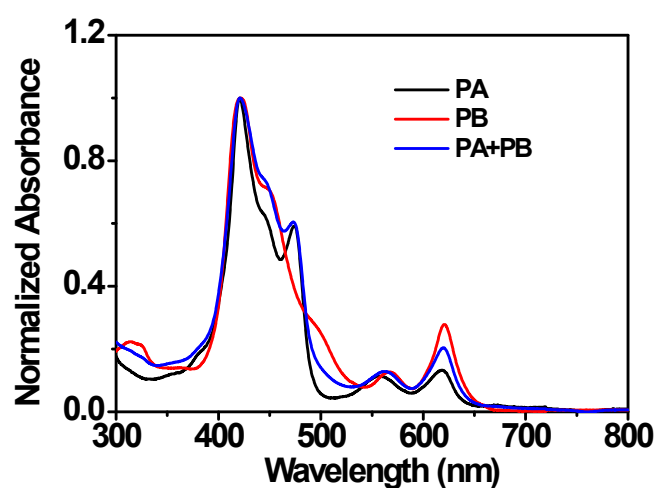


**Fig. S7** Normalized UV-vis optical absorption spectra of PA, PB and PA+PB in chloroform at a concentration of  $1 \times 10^{-5}$  M at 25 °C.

## 7. $^1\text{H}$ NMR spectral studies of PA, PB and PA+PB:

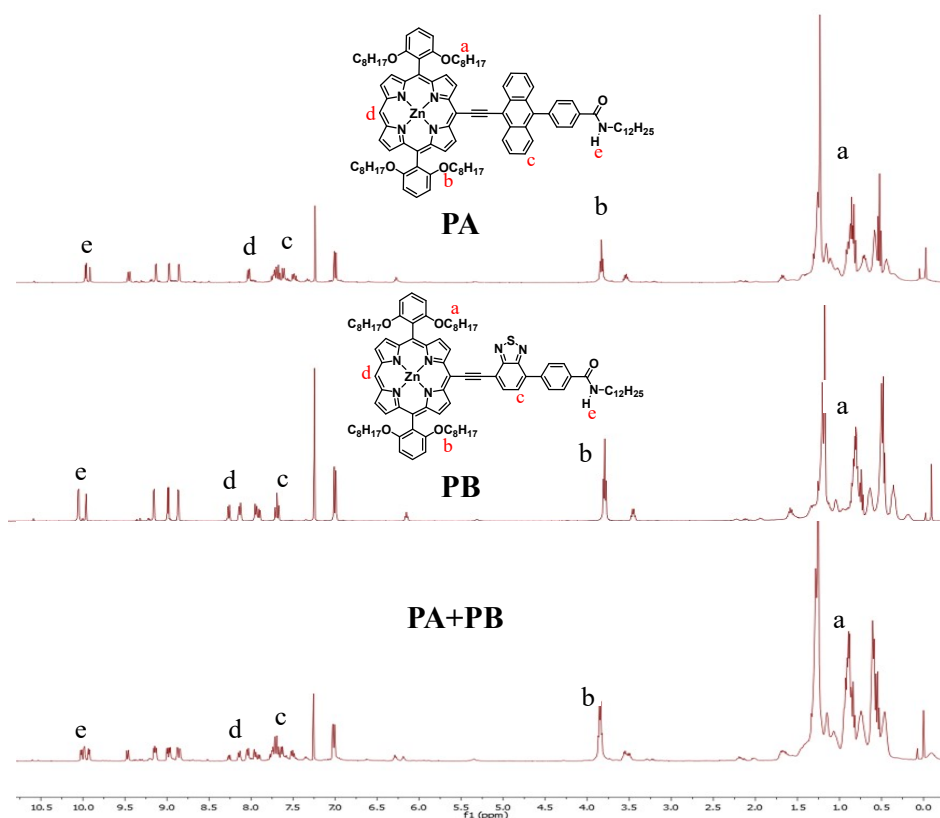


Fig. S8.  $^1\text{H}$  NMR Spectra of PA, PB and PA+PB.

## 8. NOESY spectral studies of PA, PB and PA+PB:

### 8.1. NOESY spectrum of PA:

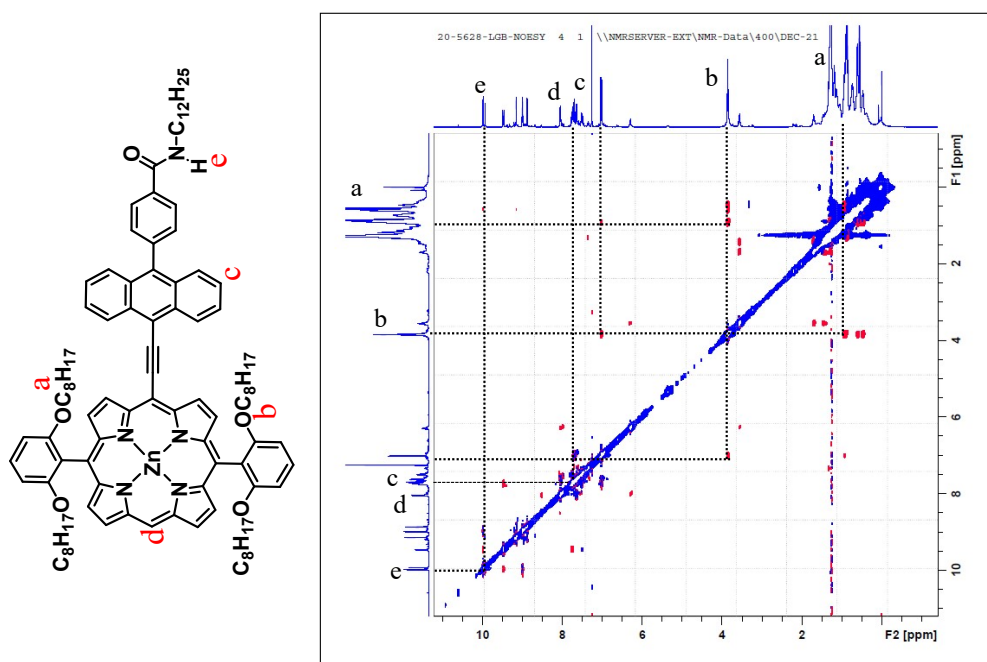


Fig. S9 NOESY spectrum of PA.

## 8.2. NOESY spectrum of PB:

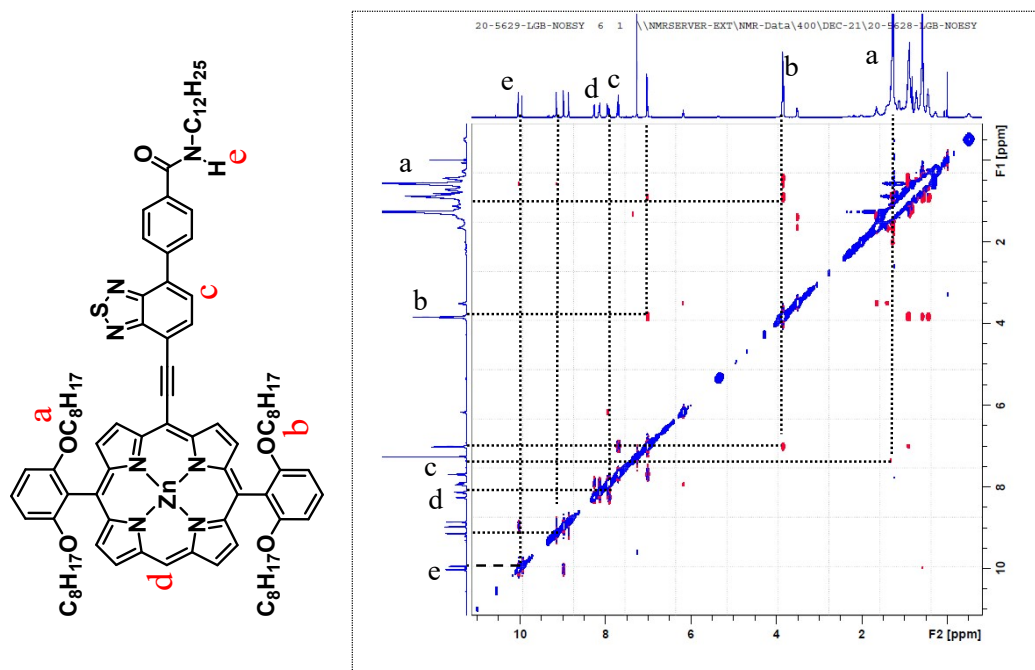


Fig. S10 NOESY spectrum of PB.

## 8.3. NOESY spectrum of PA+PB:

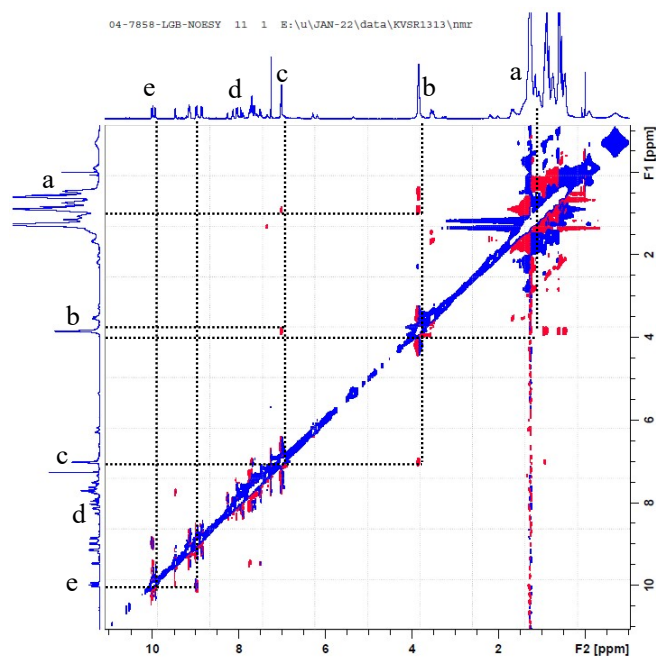


Fig. S11 NOESY spectrum of PA+PB

### 9. FT-IR studies of PA, PB and PA+PB in chloroform:

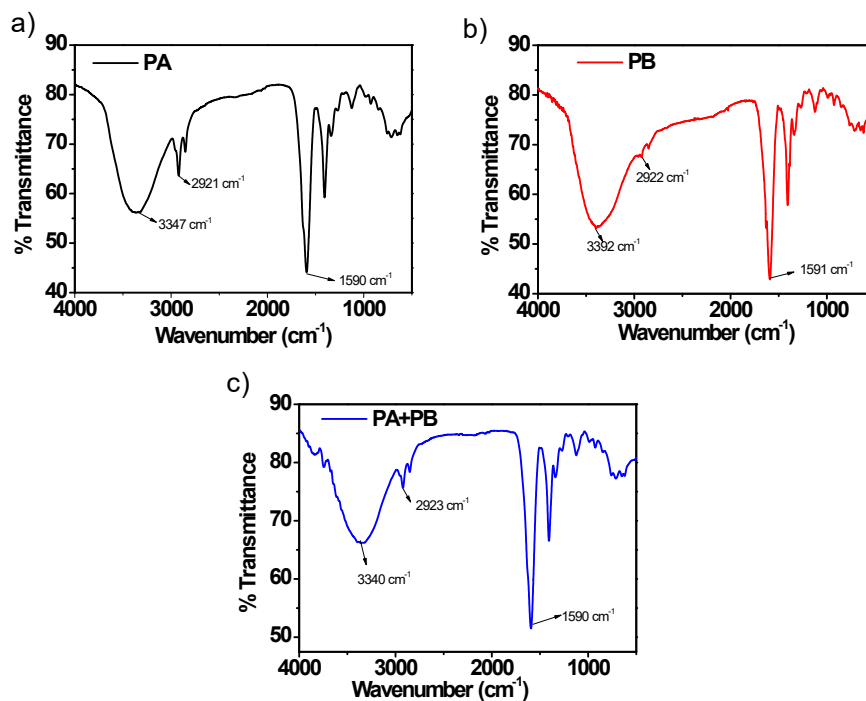


Fig. S12 FT-IR spectra of PA, PB and PA+PB in chloroform.

### 10. Electrochemistry studies of PA, PB and PA+PB:

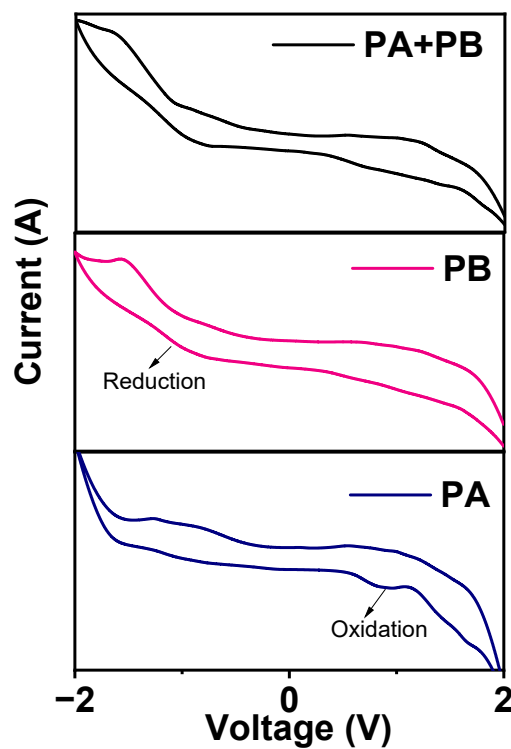
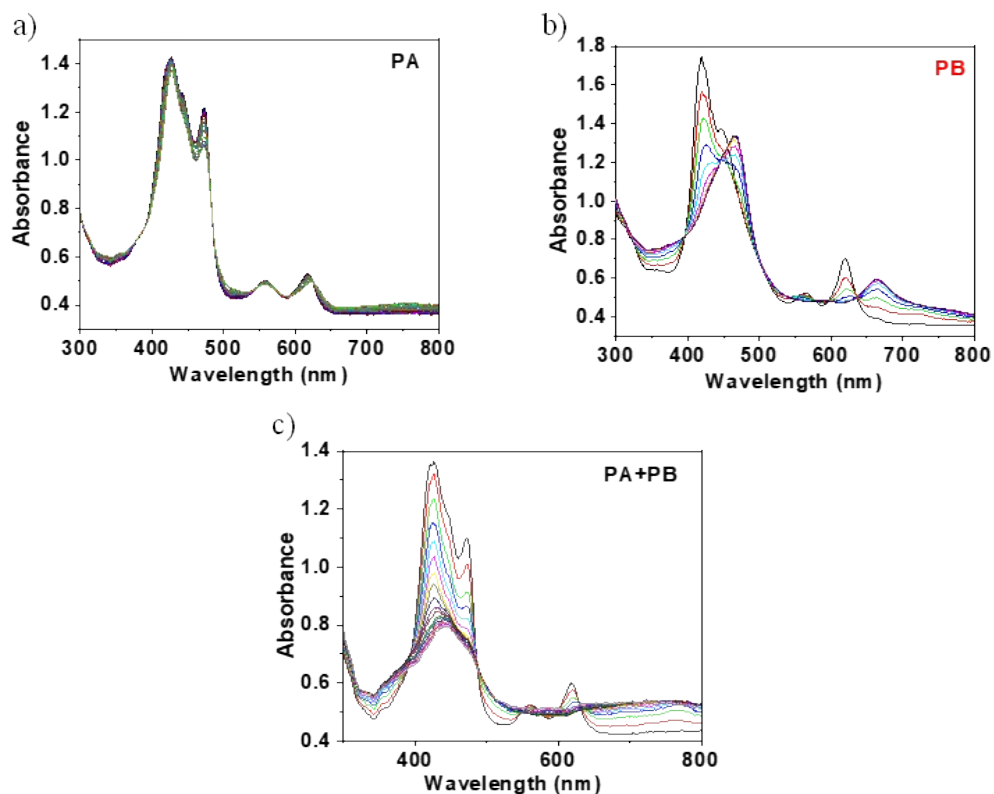


Fig. S13 Cyclic voltammetry studies of PA, PB and PA+PB



**Fig. S14** Spectro electrochemistry data of a) **PA** b) **PB** and c) **PA+PB** at 1.4 V.

**Table S1.** Photophysical and electrochemical data of **PA**, **PB** and **PA+PB** derivatives

S.No	Samples	Absorption $\lambda_{\max}(\text{nm})$	Emission $\lambda_{\text{em}}(\text{nm})$	*Lifetime (ns)		$E_{\text{Ox}}(\text{V})$	$E_{\text{Red}}(\text{V})$
				$T_1$	$T_2$		
1.	<b>PA</b>	427,613	626, 680	0.11	3.13	0.83, 1.12	-1.02, -1.23
2.	<b>PB</b>	421, 621	634, 690	6.5	5.8	0.74, 1.22	-0.80, -1.53
3.	<b>PA+PB</b>	420, 620	636, 690	0.1	1.4	0.71, 1.20	-0.82,-1.04,- 1.49

\*Lifetime values in cyclohexane

## 11. Emission studies of PA, PB and PA+PB:

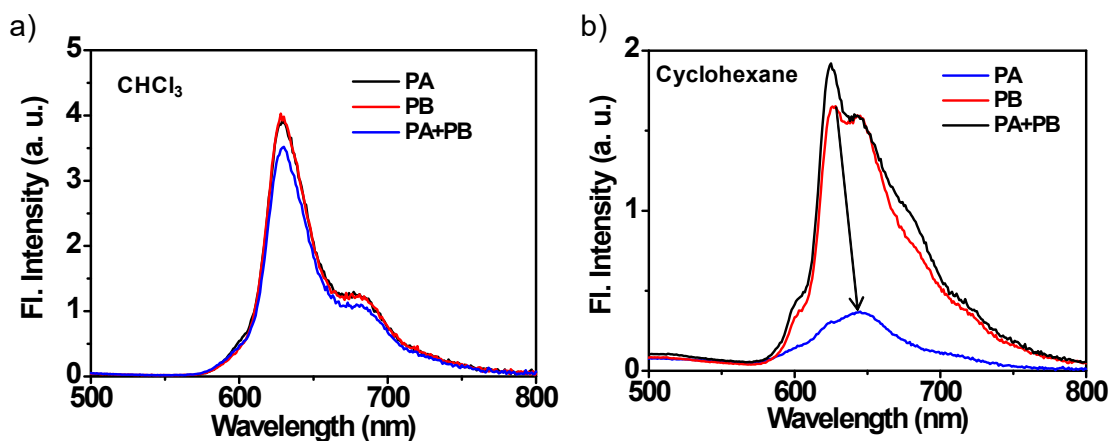


**Fig. S15** Emission spectra of PA, PB and PA+PB in a) chloroform and b) cyclohexane at an excitation wavelength of 430 nm.

### 11.1. Temperature dependent emission studies of PA, PB and PA+PB in cyclohexane:

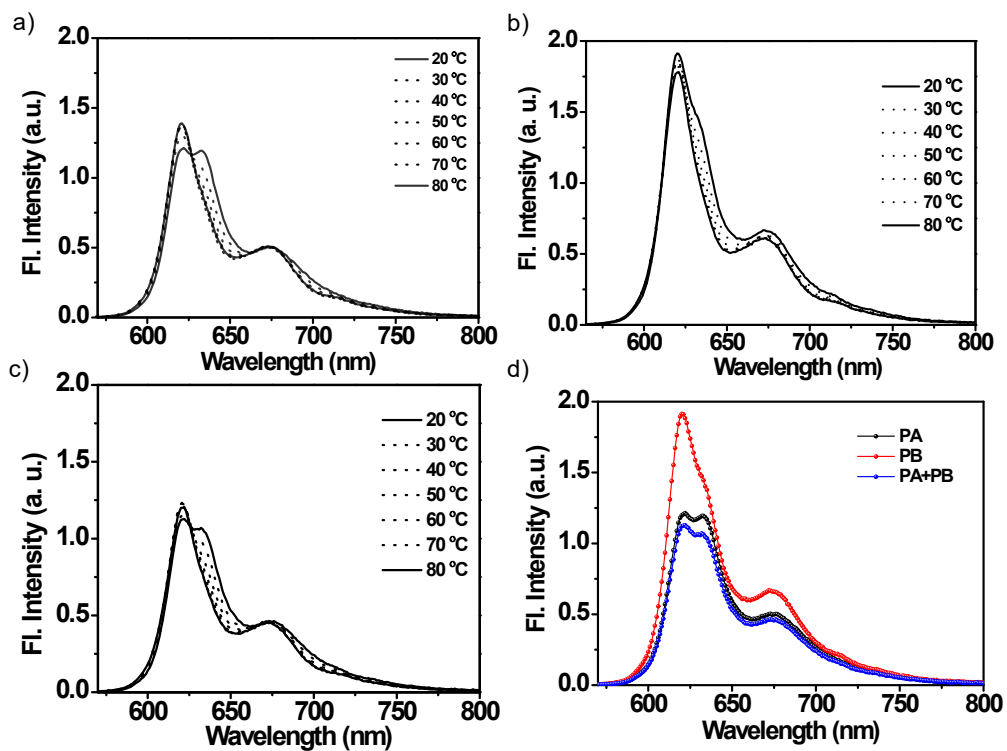


**Fig. S16** Temperature-dependent emission spectra of a-c) PA, PB and PA+PB in cyclohexane at an excitation wavelength of 430 nm. d) Emission spectra of three derivatives at 20 °C.

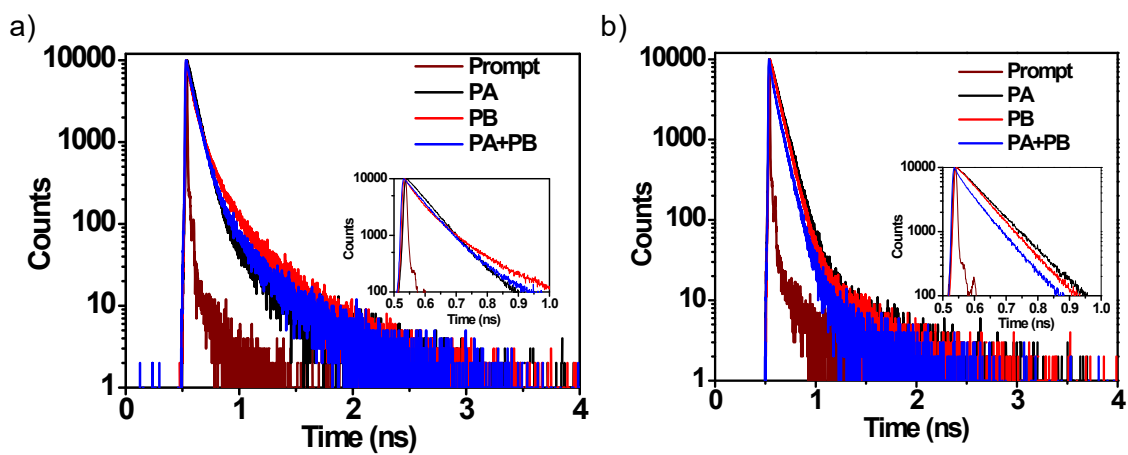


Fig. S17 Lifetime Spectra of PA, PB and PA+PB in a) Chloroform and b) Cyclohexane.

## 12. Microscopic analysis of PA+PB:

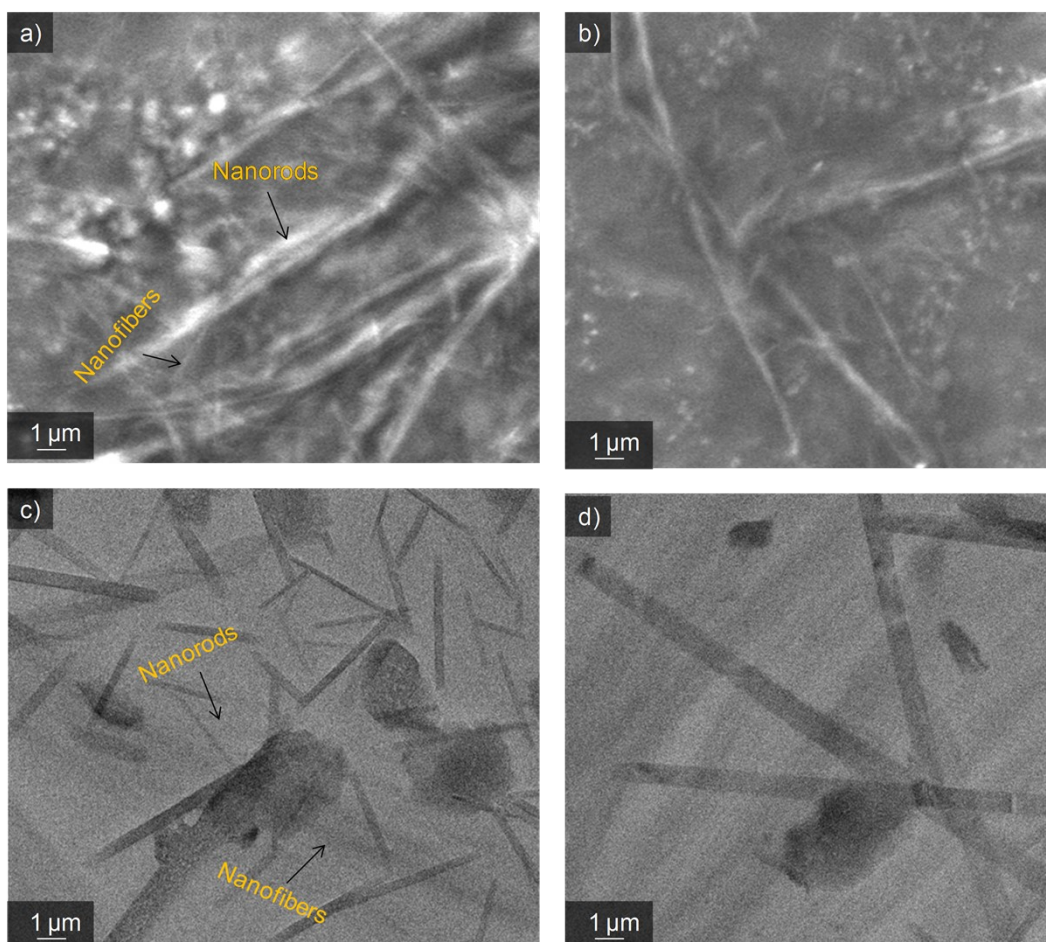


Fig. S18 a,b) SEM and c,d) TEM images of PA+PB.

### 13. Powder X-ray diffraction analyses of PA, PB and PA+PB derivatives:

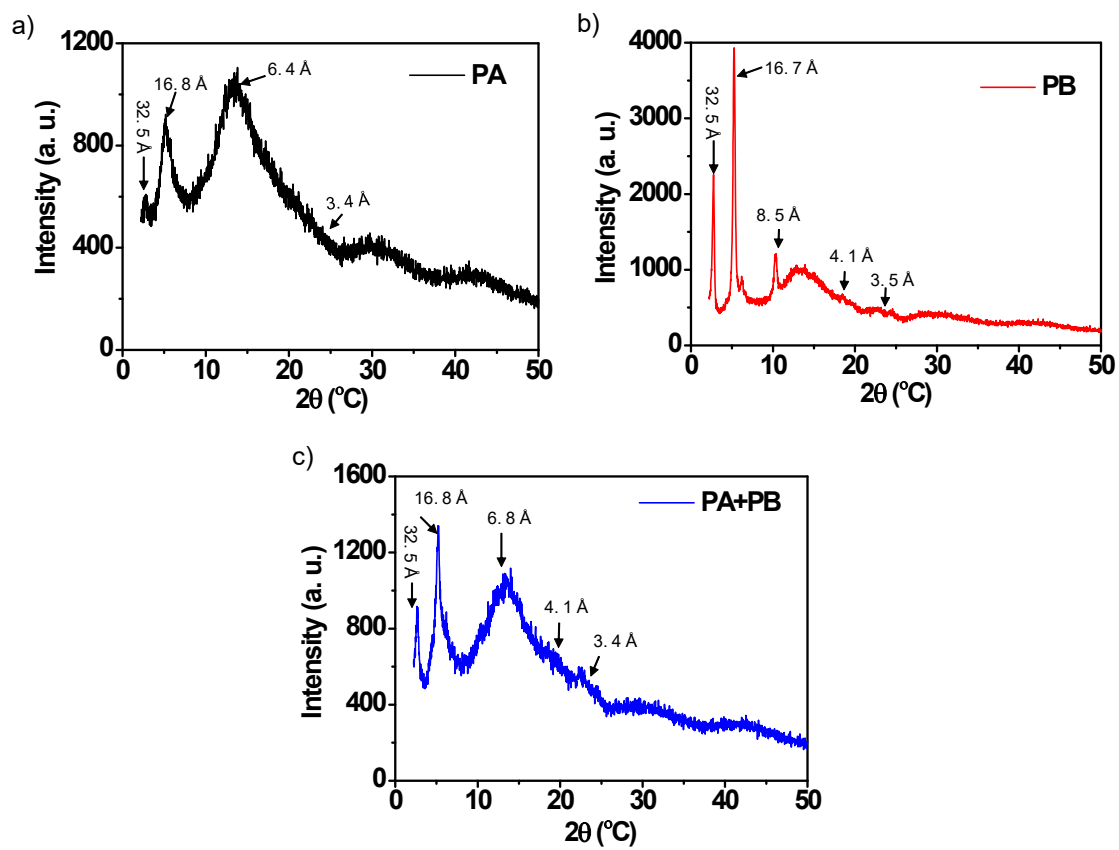
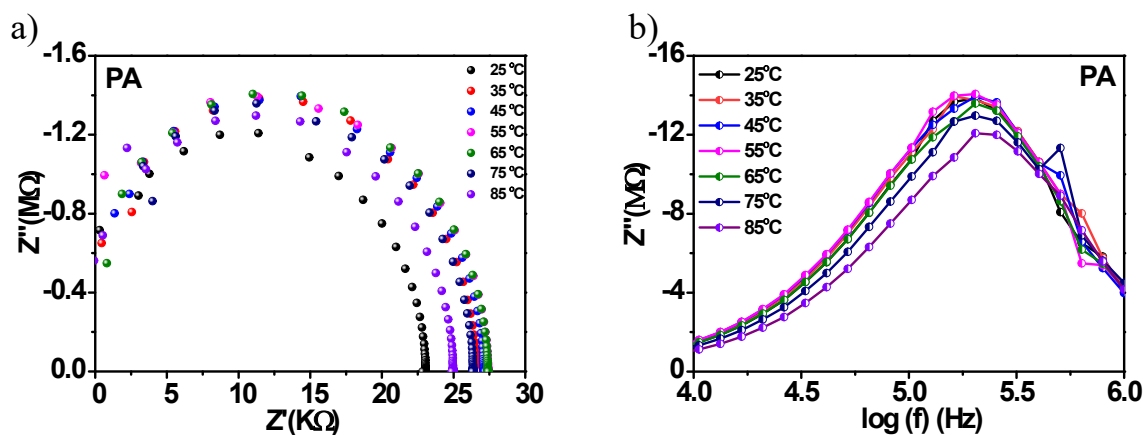


Fig. S19 Powder X-ray diffraction analyses of PA, PB and PA+PB based aggregates.

## 14. Electrochemical impedance analysis of PA, PB, and PA+PB derivatives:

### 14.1. Electrochemical Impedance Analysis of PA:



**Fig. S20** Electrochemical impedance spectral data of **PA**. (a) Temperature-dependent Nyquist plot **PA** from 25 °C to 85 °C. (b) Corresponding temperature-dependent changes of logarithmic frequency vs Imaginary impedance.

### 14.2. Electrochemical Impedance analysis of PB:

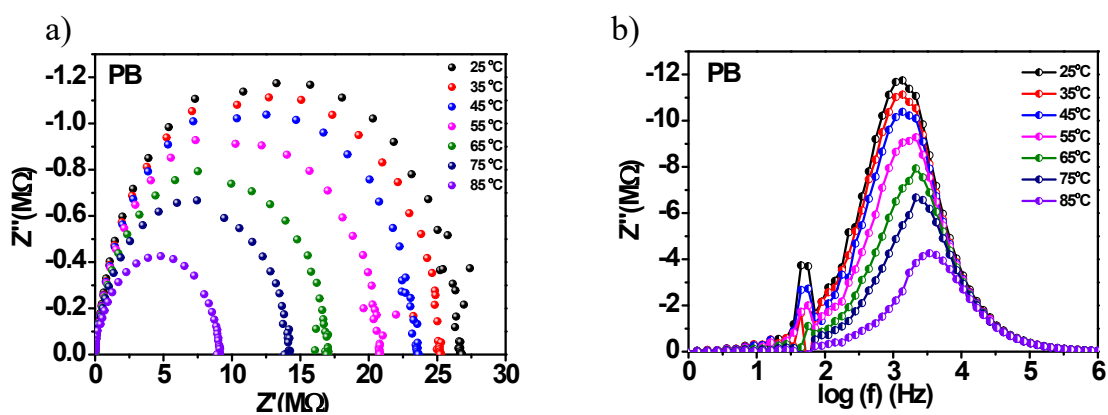


**Fig. S21** Electrochemical impedance spectral data of **PB**. (a) Temperature-dependent Nyquist plot **PB** from 25 °C to 85 °C. (b) Corresponding temperature-dependent changes of logarithmic frequency vs Imaginary impedance.

**14.3. Table S2. Summary of electrochemical impedance data of PA, PB and PA+PB:**

where,  $R_b$  = bulk resistance;  $f_p$  = bulk frequency,  $\sigma$  = specific conductivity,  $C_b$  = bulk capacitance, and  $\tau_b$  = the bulk relaxation time and estimated for the samples at variable temperatures.

Samples	T (K)	$R_b$ (M $\Omega$ )	$f_p$ (MHz)	$\sigma$ (S/cm)	$C_b$ (pF)	$\tau_b$ ( $\mu$ s)
<b>PA</b>						
	298	0.023	1.84	4.067	0.373	0.86
	308	0.026	1.62	3.516	0.378	0.97
	318	0.027	2.04	3.453	0.289	0.77
	328	0.027	1.77	3.417	0.333	0.89
	338	0.027	2.04	3.417	0.289	0.78
	348	0.026	2.03	3.555	0.302	0.78
	358	0.024	2.09	3.757	0.312	0.75
<b>PB</b>						
	298	2.66	0.0014	0.035	0.416	111.10
	308	2.49	0.0013	0.037	0.489	122.10
	318	2.35	0.0013	0.039	0.518	122.10
	328	2.07	0.0021	0.045	0.352	73.40
	338	1.69	0.0022	0.055	0.409	69.28
	348	1.40	0.0022	0.066	0.492	69.28
	358	0.90	0.0032	0.103	0.535	48.36
<b>PA+PB</b>						
	298	0.666	0.0053	0.140	0.444	29.62
	308	0.676	0.0042	0.138	0.558	37.76
	318	0.703	0.0042	0.133	0.532	37.45
	328	0.690	0.0041	0.135	0.551	38.11
	338	0.626	0.0042	0.149	0.592	37.14
	348	0.552	0.0043	0.169	0.660	36.51
	358	0.436	0.0054	0.214	0.668	29.22

#### 14. References:

1. T. Seki, S. Yagai, T. Karatsu and A. Kitamura, *J. Org. Chem.* 2008, **73**, 3328.
2. K. Sonogashira, *J. Organomet. Chem.*, 2002, **653**, 46.
3. S. Mathes, A. Yella, P. Gao, R. Humphry-Baker, B.F.E. Curchod, N. Ashari-Astani, I. Tavernelli, U. Rothlisberger, M.K. Nazeeruddin and M. Grätzel, *Nat. Chem.*, 2014, **6**, 242.
4. L. Cabau, Ch. V. Kumar, A. Moncho, J. Clifford, N. Lopez and E. A. Palomares, *Energy Environ. Sci.*, 2015, **8**, 1368.
5. N.V. Krishna, J.V.S. Krishna, S.P. Singh, L. Giribabu, L. Han, I. Bedja, R.K. Gupta and A. Islam, *J. Phys. Chem. C*, 2017, **121**, 6464.
6. S. Prasanthkumar, A. Saeki, S. Seki and A. Ajayaghosh, *J. Am. Chem. Soc.*, 2010, **132**, 8866.